Enhancing atom-field interaction in the reduced multiphoton Tavis-Cummings model

Yan Wang,[1] Jin-Lei Wu,[1] Jie Song,[1,2,3,4,*] Zi-Jing Zhang,[1] Yong-Yuan Jiang,[1,2,3,4] and Yan Xia[5]

[1]*School of Physics, Harbin Institute of Technology, Harbin 150001, China*

[2]*Key Laboratory of Micro-Nano Optoelectronic Information System, Ministry of Industry and Information Technology, Harbin 150001, China*

[3]*Key Laboratory of Micro-Optics and Photonic Technology of Heilongjiang Province, Harbin Institute of Technology, Harbin 150001, China*

[4]*Collaborative Innovation Center of Extreme Optics, Shanxi University, Taiyuan 030006, China*

[5]*Department of Physics, Fuzhou University, Fuzhou 350002, China*

(Received 24 August 2019; revised manuscript received 19 April 2020; accepted 27 April 2020; published 12 May 2020)

We propose a scheme to enhance the light-matter coupling in a cavity QED system where two Λ atoms are weakly coupled to a single-mode cavity via multiphoton interaction. By introducing a second-order nonlinear (parametric) driving of the cavity, the original N-photon exchanges between the atoms, and the cavity can be reduced to either an effective single- or two-photon transition depending on the odevity of N, with the effective atom-field interaction strength being significantly enhanced. This results in an N-dependent effective coupling strength on top of the exponential enhancement induced only by the parametric driving. As an example, we demonstrate that our proposal can be exploited for the preparation of high-fidelity steady-state entanglement. The proposed scheme could provide a feasible alternative for diverse applications in quantum technologies.

DOI: 10.1103/PhysRevA.101.053826

I. INTRODUCTION

The Jaynes-Cummings (JC) model of a two-level atom interacting with a single-mode bosonic field under rotating-wave approximation (RWA) has been a research interest in the field of quantum optics [1–7]. An extended JC model considering multiphoton exchanges is known as the multiphoton JC model, where the transition between the upper and lower levels of the atom may involve m ($\geqslant 2$) photons if the energy separation between the levels is close to the energy of m quanta of the electromagnetic field [8–11]. As a simplest nonlinear generalization, the two-photon JC model has been extensively studied [12–14]. It has been demonstrated that two-photon JC Hamiltonian can be achieved in many physical architectures, such as optical and microwave cavities [15,16], the trapped-ion domain [17,18], and superconducting circuits [19–22].

Generalizing the JC model to the n (>1) atom case leads to the so-called Tavis-Cummings (TC) model [23,24]. Although it seems a straightforward extension of the JC model, the TC model has gained renewed interest since it provides a framework for exploring intrinsically multiqubit properties [25]. In analogy with the multiphoton JC model, the TC model has been generalized to include multiphoton processes [26]. The TC model exhibits a wide variety of interesting phenomena [27–30] and can be exploited to implement quantum-information protocols, in particular quantum entanglement [31,32]. The atom-field entanglement in the two-atom TC model has been studied for single-photon transitions [33] as well as nondegenerate [34] or degenerate [35] two-photon transitions.

Reaching the light-matter strong coupling regime (SCR) has been the subject of many theoretical and experimental works in atomic physics and quantum optics and has driven the field of cavity quantum electrodynamics (QED) [36–42]. The SCR, which enables a high degree of manipulation and control of quantum systems, is prerequisite for implementing quantum information tasks [43,44]. To date, considerable efforts have been devoted to enhancing light-matter coupling to reach the SCR. Very recently, it was demonstrated that parametric driving of the cavity mode can be used to exponentially enhance the effective coupling in the qubit-cavity system [45–47] and optomechanical system [48–51]. In this paper, inspired directly by the achievements in Refs. [45,46], we generalize and explore an intriguing method to enhance the atom-field coupling using parametric driving of a cavity. Different from previous proposals for coupling enhancement, we herein consider a multiphoton TC system, where two Λ atoms are coupled to a single-mode cavity via N-photon interaction. We show that the effective atom-field coupling strength can be enhanced to be N-dependent on top of the exponential enhancement induced only by the parametric driving. Then the effects of dissipation on the evolution of system are discussed. Numerical results show that with increasing N the detrimental effects of dissipation can be mitigated, resulting in significant recovery of population oscillations. Moreover, as a straightforward application, we also investigate the generation of a maximally entangled steady state between atoms. For entanglement preparation, it is well known that high-fidelity F requires high cooperativity C, according to $1-F \propto C^{-1/2}$ [52,53]. Due to the effective enhancement of C, we demonstrate that high-fidelity steady-state entanglement is achievable in the proposed scheme.

The remainder of the paper is structured as follows. In Sec. II we describe the physical model and give the

*jsong@hit.edu.cn

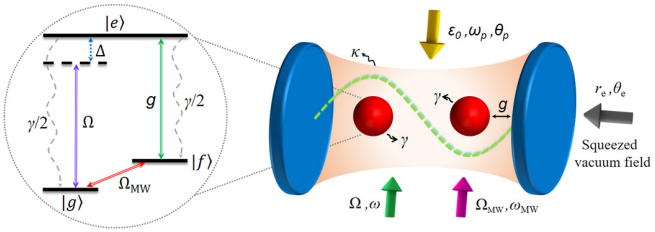

FIG. 1. Schematic of the proposed cavity QED system. Two identical Λ atoms are trapped into a single-mode cavity, which is parametrically driven by a second-order nonlinear field with strength ϵ_0, frequency ω_p, and phase θ_p. A broadband squeezed vacuum field with squeezing parameter r_e and reference phase θ_e is injected into the cavity, which can be approximated as a squeezed vacuum reservoir. As depicted in the leftward inset, the cavity mode couples the $|e\rangle \leftrightarrow |f\rangle$ transition with strength g. A laser field with frequency ω and Rabi frequency Ω drives the $|g\rangle \leftrightarrow |e\rangle$ transition, and a microwave field with frequency $\omega_{\rm MW}$ and Rabi frequency $\Omega_{\rm MW}$ drives the $|g\rangle \leftrightarrow |f\rangle$ transition. We assume that the atomic spontaneous emission rates are $\gamma/2$, and the cavity decay rate is κ.

corresponding Hamiltonian of the system. In Sec. III we first reduce the N-photon TC Hamiltonian to obtain the effective Hamiltonians describing the reduced single- and two-photon interactions. Then we verify the validity of the model by numerically analyzing the dynamical evolutions of the system. As a simple application, we demonstrate in Sec. IV that the proposed scheme can be exploited for high-fidelity steady-state entanglement preparation. Finally, we give a brief discussion of experimental implementations and summarize our conclusions in Sec. V.

II. THE SYSTEM AND HAMILTONIAN

We consider a cavity QED (CQED) system consisting of two identical Λ atoms trapped into a single-mode cavity, as depicted in Fig. 1. The energy-level diagram of the atom is shown in the inset of Fig. 1. Each atom has two ground states $|g\rangle$ and $|f\rangle$ and one excited state $|e\rangle$ with the corresponding energies ω_g, ω_f, and ω_e, respectively. The transition between the states $|g\rangle$ and $|e\rangle$ is driven via a laser field with frequency ω and Rabi frequency Ω, while the transition between the states $|g\rangle$ and $|f\rangle$ is driven via a microwave field with frequency $\omega_{\rm MW}$ and Rabi frequency $\Omega_{\rm MW}$. In particular, the transition between states $|f\rangle$ and $|e\rangle$ is coupled to the cavity mode with coupling constant g via N-photon degenerate interaction, i.e., coherent exchange of N excitations of the cavity mode with the atom [8,9,26]. A second-order nonlinear (i.e., parametric) driving field [11,16,45,54,55] of amplitude ϵ_0, single-photon frequency ω_p, and phase θ_p is employed to squeeze the cavity mode [45,49,51]. We point out that the laser and microwave fields are introduced intentionally in our scheme for implementing dissipative entanglement generation. Also, to eliminate completely the additional noise induced by the parametric driving for high-fidelity entanglement generation, a broadband squeezed vacuum field is injected into the cavity, as we detail in Sec. IV.

Given the above setups, the Hamiltonian determining the unitary dynamics of the system is given by

$$H = H_{\rm AC}^{(N)} + H_{\rm CL} + H_{\rm MW}, \tag{1}$$

where

$$\begin{aligned} H_{\rm AC}^{(N)} &= \omega_0 a^\dagger a + \sum_{k=1,2} \{\omega_e |e\rangle_k\langle e| + \omega_f |f\rangle_k\langle f| \\ &\quad + \omega_g |g\rangle_k\langle g| + g[|e\rangle_k\langle f| a^N + (a^\dagger)^N |f\rangle_k\langle e|]\} \\ &\quad + \epsilon_0[a^2 e^{i(2\omega_p t-\theta_p)} + (a^\dagger)^2 e^{-i(2\omega_p t-\theta_p)}], \\ H_{\rm CL} &= \frac{\Omega}{2} e^{i\omega t} \sum_{k=1,2} (-1)^{k-1} |g\rangle_k\langle e| + \text{H.c.}, \\ H_{\rm MW} &= \frac{\Omega_{\rm MW}}{2} e^{i\omega_{\rm MW} t} \sum_{k=1,2} |g\rangle_k\langle f| + \text{H.c.} \end{aligned} \tag{2}$$

Here $H_{\rm AC}^{(N)}$ denotes the degenerate N-photon two-atom TC Hamiltonian containing nonlinear driving terms, $H_{\rm CL}$ ($H_{\rm MW}$) is Hamiltonian describing the interaction between laser field (microwave field) and atoms, and a ($a^\dagger$) is the annihilation (creation) operator of the cavity mode with frequency ω_0.

III. REDUCING N-PHOTON TC HAMILTONIAN FOR ENHANCING ATOM-CAVITY COUPLING

In this section, we merely focus on the atom-cavity coupling and assume for the moment that the laser and microwave fields, as well as the squeezed vacuum field, are all turned off, i.e., $\Omega = \Omega_{\rm MW} = r_e = 0$.

A. Derivation of the effective Hamiltonian

First, we demonstrate how the degenerate N-photon TC Hamiltonian is reduced in the presence of the nonlinear driving field, yielding prominent enhancement in atom-cavity coupling simultaneously. Specifically, by choosing separate parameter conditions in terms of the odevity of the photon number N, the original N-photon TC Hamiltonian can be reduced to either an effective single- or two-photon TC Hamiltonian which corresponds to odd or even N, respectively. Moreover, the resulting effective coupling strengths between atom and cavity field can be enhanced greatly. Based on calculation and derivation (see Appendix A for details), we obtain effective form of the reduced single- and two-photon TC Hamiltonians

$$\begin{aligned} H_{\rm ACS}^{(N_o)} &= \Delta_s a^\dagger a + \sum_{k=1,2} \Big\{ \Delta_e^{(N_o)} |e\rangle_k\langle e| + \omega_f |f\rangle_k\langle f| \\ &\quad + (-V)^m U^{m+1} g |e\rangle_k\langle f| \sum_l P_l [a^{m+1} (a^\dagger)^m] \\ &\quad + \text{H.c.} \Big\}, \end{aligned} \tag{3a}$$

$$\begin{aligned} H_{\rm ACS}^{(N_e)} &= \Delta_s a^\dagger a + \sum_{k=1,2} \Big\{ \Delta_e^{(N_e)} |e\rangle_k\langle e| + \omega_f |f\rangle_k\langle f| \\ &\quad + (-V)^n U^{n+2} g |e\rangle_k\langle f| \sum_l P_l [a^{n+2} (a^\dagger)^n] \\ &\quad + \text{H.c.} \Big\}, \end{aligned} \tag{3b}$$

which are valid for $\Delta_e^{(N_o)} - \omega_f = \Delta_s$ and $\Delta_e^{(N_e)} - \omega_f = 2\Delta_s$, respectively. In fact, the Hamiltonian in Eq. (3) has been transformed to the squeezed reference frame via a squeezing transformation. In Eq. (3) N_o and N_e denote odd and even photon numbers, respectively; $\Delta_e^{(N)} = \omega_e - N\omega_p$; $U = \cosh(r_p)$, $V = \sinh(r_p)$, where $r_p = (1/2)\text{arctanh}(2\epsilon_0/\Delta_p)$ with $\Delta_p = \omega_0 - \omega_p$; $\Delta_s = \Delta_p \text{sech}(2r_p)$; $m = \frac{N_o-1}{2}$, $n = \frac{N_e-2}{2}$. The sum with respect to l is over all permutations (produced by the permutation operator P_l) with m (n) photon creation operators; e.g., for $N_o = 3$, $P_l[a^2a^\dagger]$ generates three permutations $\{a^2a^\dagger, a^\dagger a^2, aa^\dagger a\}$. Notably, the atom-field coupling is effectively enhanced compared to the original coupling strength g, i.e., the effective coupling constants become dependent on the photon number N on top of the exponential enhancement with respect to r_p.

The full permutations with respect to operators a and $a^\dagger$ in the interactions terms of Eq. (3) can be simplified by using the commutation relation $[a, a^\dagger] = 1$. Without loss of generality, we herein take $N = 1, 2, 3, 4$ as examples. The corresponding simplified Hamiltonians are derived, respectively, as

$$H_{\text{ACS}}^{(1)} = \Delta_s a^\dagger a + \sum_{k=1,2} \left[\Delta_e^{(1)} |e\rangle_k\langle e| + \omega_f |f\rangle_k\langle f| + (gU|e\rangle_k\langle f|a + \text{H.c.})\right], \tag{4}$$

$$H_{\text{ACS}}^{(2)} = \Delta_s a^\dagger a + \sum_{k=1,2} \left[\Delta_e^{(2)} |e\rangle_k\langle e| + \omega_f |f\rangle_k\langle f| + (gU^2|e\rangle_k\langle f|a^2 + \text{H.c.})\right], \tag{5}$$

$$H_{\text{ACS}}^{(3)} = \Delta_s a^\dagger a + \sum_{k=1,2} \left[\Delta_e^{(3)} |e\rangle_k\langle e| + \omega_f |f\rangle_k\langle f| - (3gU^2V|e\rangle_k\langle f|aa^\dagger a + \text{H.c.})\right], \tag{6}$$

$$H_{\text{ACS}}^{(4)} = \Delta_s a^\dagger a + \sum_{k=1,2} \left\{\Delta_e^{(4)} |e\rangle_k\langle e| + \omega_f |f\rangle_k\langle f| - [gU^3V|e\rangle_k\langle f|(4aa^\dagger a^2 + 2a^2) + \text{H.c.}]\right\}. \tag{7}$$

Also, we assume that one atom is initially populated on the excited state $|e\rangle$, whereas another one is populated on the ground state $|g\rangle$, and the initial state of the cavity mode is a n_p-photon Fock state. Then the effective Hamiltonians given by Eqs. (6) and (7) can be further simplified as

$$H_{\text{ACS}}^{(3)} = \Delta_s a^\dagger a + \sum_{k=1,2} \left\{\Delta_e^{(3)} |e\rangle_k\langle e| + \omega_f |f\rangle_k\langle f| - [3(n_p+1)gU^2V|e\rangle_k\langle f|a + \text{H.c.}]\right\} \tag{8}$$

and

$$H_{\text{ACS}}^{(4)} = \Delta_s a^\dagger a + \sum_{k=1,2} \left\{\Delta_e^{(4)} |e\rangle_k\langle e| + \omega_f |f\rangle_k\langle f| - [(4n_p+6)gU^3V|e\rangle_k\langle f|a^2 + \text{H.c.}]\right\}. \tag{9}$$

In fact, we have simplified the interaction terms in the Hamiltonians (6) and (7) by using the simple operator a and a^2 to describe the effective single- and two-photon processes, respectively. In addition, for another initial state of $|f\rangle_1|g\rangle_2|n_p\rangle_c$ (or $|g\rangle_1|f\rangle_2|n_p\rangle_c$), the effective atom-cavity coupling strengths in Eqs. (8) and (9) will be $3n_pgU^2V$ and $(4n_p - 2)gU^3V$, respectively.

An interesting situation can be observed directly in Eqs. (4), (5), (8), and (9), in which the original N-photon TC Hamiltonian is reduced to either an effective single- or two-photon TC Hamiltonian, depending entirely on the odevity of N. For $N = 1$ [see Eq. (4)], an exponentially enhanced coupling is achievable, corresponding to a coupling strength of $g\cosh(r_p)$. We note that similar results (for $N = 1$) have been demonstrated in several typical works [45–47] and generalized in our recent work [56,57]. In principle, this exponential enhancement can be understood as follow: The parametric drive modifies the eigenstates of the cavity Hamiltonian, which convert to squeezed photons with amplified fluctuations, hence causing a larger interaction with the atoms [45]. Nevertheless, further enhancement of coupling is expected in the present scheme. For instance, the coupling strength could be enhanced to $3g\cosh^2(r_p)\sinh(r_p)$ for $N = 3$ and $n_p = 0$, which is about 5.4 times higher than that for $N = 1$ when a small r_p of 1 is chosen. Note that the coupling enhancement in our scheme is distinct from the $\sqrt{N!}$ enhancement associated with the N-photon atom-cavity interaction without using the parametric driving field. In addition, large r_p corresponds to extremely strong driving field amplitude ϵ_0, which may cause problems in experimental implementation [47]. In this sense the advantage of the proposed scheme seems apparent, i.e., relatively large r_p is no longer necessary for achieving sufficient enhancement in coupling strength. Proposing such an alternative scheme for enhancing atom-field coupling is one of our important results.

B. Dynamical evolution

The above-mentioned properties can be understood more clearly by exploring the dynamical evolution of the system. Here the effects of dissipation are not considered because it does not affect current analysis for system performance. In this case, the dynamical evolution of the system can be described by the quantum Liouville equation $\dot{\rho} = i[\rho, H_{\text{ACS}}^{(N)}]$, where $H_{\text{ACS}}^{(N)}$ is the exact Hamiltonian given by Eq. (A3). We assume that the initial states of two atoms and cavity mode are excited state $|e\rangle_1$, ground state $|g\rangle_2$, and vacuum state $|0\rangle_c$, respectively. Note that as this is a vacuum state in the squeezed frame, in the original laboratory frame the state will correspond to a squeezed vacuum state. Experimentally, this specific initial cavity state can be produced, e.g., in the optical domain, via degenerated parametric down-conversion in the optical parametric amplifier [58–60]; or, in the microwave domain, via a Josephson parametric amplifier based on the nonlinearity Josephson junctions [61–64].

By numerically solving the Liouville equation, we obtain the time evolution of the population for the first atom being in the excited state $P_e(t)$ [65]. Figure 2(a) shows the corresponding results for cases of $N_o = 1, 3$, where we choose the parameter condition $\Delta_e^{(N_o)} - \omega_f = \Delta_s$. Ideal oscillations can be observed, indicating coherent energy exchange between the atom and the cavity photon field. Moreover, the obvious shrinking of the oscillation period for larger N_o is a direct evidence of the enhancement in effective coupling strength. For cases of $N_e = 2, 4$ similar situations appear as shown in

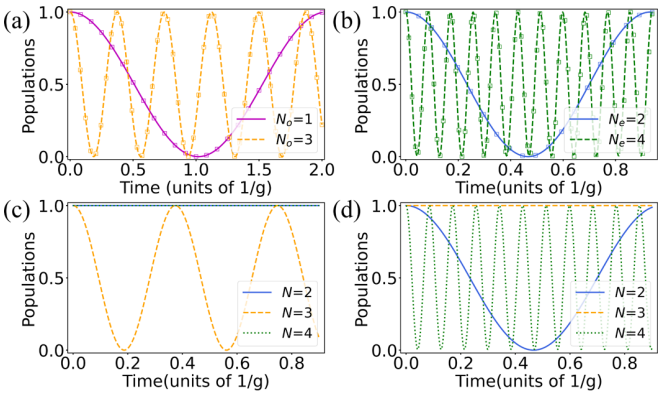

FIG. 2. Time evolution of the population for the first atom being in the excited state. The curves and the hollow squares are obtained from exact and effective Hamiltonians, respectively. The parameters are $r_p = 1$, (a, c) $\Delta_e - \omega_f = \Delta_s = 5 \times 10^3 g$, (b, d) $\Delta_e - \omega_f = 2\Delta_s = 5 \times 10^3 g$. The initial state of the system is $|e\rangle_1|g\rangle_2|0\rangle_c$, which is in resonance with state $|f\rangle_1|g\rangle_2|1\rangle_c$ ($|f\rangle_1|g\rangle_2|2\rangle_c$) via single-photon (two-photon) interaction. Dissipation is neglected.

Fig. 2(b), in which we choose the different parameter condition $\Delta_e^{(N_e)} - \omega_f = 2\Delta_s$. In both figures, the analytical results marked by hollow squares are obtained from the effective Hamiltonians given by Eqs. (4), (5), (8), and (9) ($n_p = 0$). Clearly, the analytical results are in excellent agreement with the exact numerical results. For the same condition $\Delta_e^{(N_o)} - \omega_f = \Delta_s$, the time evolution of $P_e(t)$ for $N = 2, 3, 4$ is plotted in Fig. 2(c). It can be seen that the atom always stays on the excited state for even N ($N_e = 2, 4$). This is reasonable because the unmatched parameter condition introduces large detunings into the transition paths of atom, hence completely prohibiting the oscillations of the excited state. As for the condition $\Delta_e^{(N_e)} - \omega_f = 2\Delta_s$, the situation is contrary to that in Fig. 2(c), where the oscillation for odd N is suppressed, as observed in Fig. 2(d).

To further demonstrate the effective single- or two-photon interaction in the reduced N-photon Hamiltonian, we plot the time evolution of $P_e(t)$ with a different initial state of the cavity mode, as shown in Fig. 3. Here we assume that two atoms are initially in their ground states $|f\rangle_1$ and $|g\rangle_2$, respectively. For one photon initially populated in the cavity mode [see Fig. 3(a)], only oscillation for $N = 3$ can be observed, revealing that the atom interacts with the cavity photon via sn effective single-photon process. When, however, two photons are initially populated in the cavity mode [see Fig. 3(b)], all oscillations for $N = 2, 3, 4$ are observed. This indicates that, for $N = 2, 4$ (more precisely, even N), at least two photons are required for the transitions of atom. Further, for arbitrary even N the transitions of the atom can be triggered as long as two photons initially populated in the cavity.

C. Effects of dissipation

We now take the cavity and atom dissipation into consideration. In the squeezed frame, the master equation describing only the dynamics of the atom-cavity-coupling system is

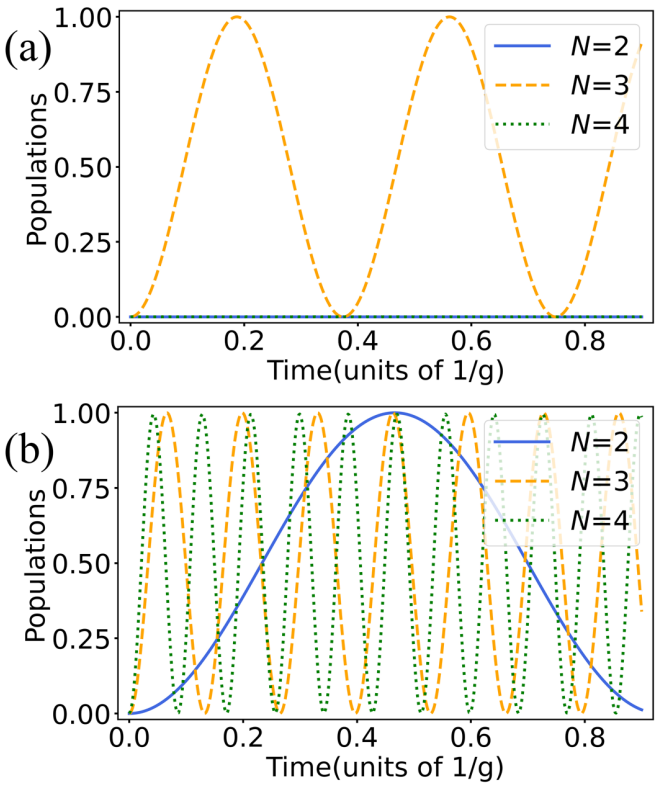

FIG. 3. Time evolution of the population for the first atom being in the excited state. The results are obtained from the exact Hamiltonian. The common parameters are $r_p = 1$, $\Delta_e - \omega_f = \Delta_s = 5 \times 10^3 g$ for $N = 3$, and $\Delta_e - \omega_f = 2\Delta_s = 5 \times 10^3 g$ for $N = 2, 4$. The initial states of the system are (a) $|f\rangle_1|g\rangle_2|1\rangle_c$ and (b) $|f\rangle_1|g\rangle_2|2\rangle_c$, respectively. Dissipation is neglected.

given by

$$\dot{\rho} = i[\rho, H_{\rm ACS}^{(N)}] + \sum_{z,k} \mathcal{L}(L_{zk})\rho + (N_s + 1)\mathcal{L}(L_a)\rho + N_s\mathcal{L}(L_a^\dagger)\rho - M_s\mathcal{L}'(L_a^\dagger)\rho - M_s^*\mathcal{L}'(L_a)\rho, \quad (10)$$

where $L_{zk} = \sqrt{\gamma/2}|z\rangle_k\langle e|$ ($z = g, f$) are the Lindblad operators describing the atomic spontaneous emissions with identical rate $\gamma/2$, $L_a = \sqrt{\kappa}a$ is the Lindblad operator describing the cavity decay with rate κ, $\mathcal{L}(o)\rho = o\rho o^\dagger - (o^\dagger o\rho + \rho o^\dagger o)/2$, $\mathcal{L}'(o)\rho = o\rho o - (oo\rho + \rho oo)/2$, and $N_s = \sinh^2(r_p)$ and $M_s = \cosh(r_p)\sinh(r_p)$ describe the squeezing-induced noise, corresponding to the thermal noise and two-photon correlation strengths [48,66], respectively. In Fig. 4 we plot the time evolution of $P_e(t)$ in the first five periods by numerically solving master equation (10) with $N = 1, 2, 3$, and 4. The horizontal time axis has been rescaled in terms of respective period of oscillation for various N (T_N). Actually, the value of T_N decreases with increasing N. The cavity and atomic decay rates are set as $\kappa = \gamma/2 = 0.1g$. As shown in Fig. 4(a), the amplitude of oscillations is strongly suppressed for $N = 1$ where the maximum of population $P_e(t)$ during the second period is approximate to 0.6. Increasing N to 2 can enhance the effective coupling strength (nearly 3.3 times in comparison with that for $N = 1$), thus resulting

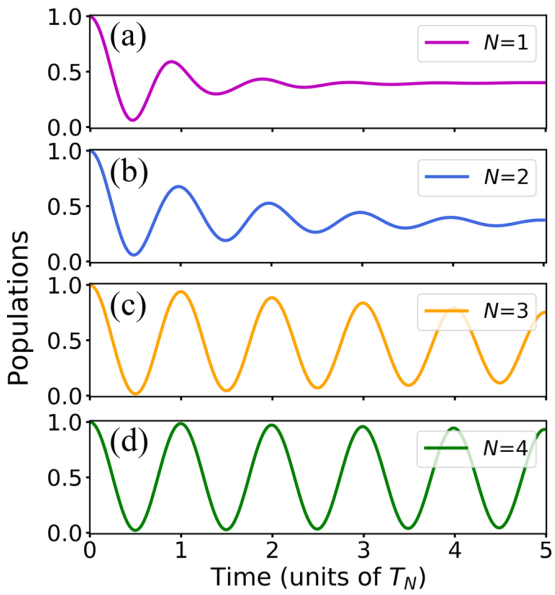

FIG. 4. The effects of dissipation on the time evolution of $P_e(t)$. Here population oscillations in the first five periods for N from 1 (top) to 4 (bottom) are plotted. The unit of the horizontal axis T_N denotes the period of oscillation for various N, and it decreases with increasing N. Other parameters are $r_p = 1.5$, $\kappa = \gamma/2 = 0.1g$, $\Delta_e - \omega_f = \Delta_s = 2 \times 10^4 g$ for $N = 1, 3$, and $\Delta_e - \omega_f = 2\Delta_s = 2 \times 10^4 g$ for $N = 2, 4$. The initial state of the system is $|e\rangle_1|g\rangle_2|0\rangle_c$.

in modest recovery of oscillation, as observed in Fig. 4(b). Since for larger N the effective coupling can be enhanced greatly, we expect that the detrimental effects of dissipation will be further mitigated for $N = 3$ and 4. As illustrated in Figs. 4(c) and 4(d), significant recovery of oscillations can be clearly observed, revealing that the effective coupling strengths for $N = 3, 4$ are large enough to overwhelm the strong dissipation. Notably, for $N = 4$, the maximum of $P_e(t)$ after the fifth period of oscillation is still above 0.9.

IV. ENHANCED STEADY-STATE ENTANGLEMENT

The enhancement of effective atom-cavity coupling offers great potential for generation of high-fidelity (F) steady-state entanglement. For the proposed N-photon model, the higher the power N, the larger the enhancement of effective coupling. In this sense, it is convenient to select larger N to achieve higher C [according to $C = g^2/(\kappa\gamma)$] and therefore F. Given that there is a trade-off between the coupling enhancement and the feasible parameters selection, in this section we mainly demonstrate the improvement of entanglement preparation in the model with $N = 3$. Simultaneously, for generating high-fidelity steady-state entanglement, the additional noise [i.e., thermal noise and two-photon correlation, as described in Eq. (10)] induced by the parametric driving needs to be eliminated. For this purpose, we introduce a squeezed vacuum field to drive the cavity mode, such that the undesired noise could be completely suppressed as long as specific phase matching is satisfied (see Appendix B for details). In fact, this ensures the cavity mode in the squeezed frame will equivalently interact with a vacuum reservoir. The dynamics of the system is thus governed by the standard master equation in the Lindblad form $\dot{\rho} = i[\rho, H'] + \sum_{z,k} \mathcal{L}(L_{zk})\rho + \mathcal{L}(L_a)\rho$. The detailed derivation regarding this master equation is given in Appendix B.

We now turn to some principle insights with respect to the dissipative entanglement preparation in our scheme. Specifically, inspired by the standard procedure in Refs. [46,53,67], we rewrite the system Hamiltonian for $N = 3$ in the squeezed frame as

$$H'' = H_g + H_e + V_+ + V_-, \tag{11}$$

where

$$\begin{aligned} H_g &= \sum_{k=1,2}\left[\omega_f|f\rangle_k\langle f| + \frac{\Omega_{\rm MW}}{2}(e^{i\omega_{\rm MW}t}|g\rangle_k\langle f| + \text{H.c.})\right], \\ H_e &= \Delta_s a^\dagger a + \sum_{k=1,2}\left[\Delta_e^{(3)}|e\rangle_k\langle e| - (g_{\rm eff}|e\rangle_k\langle f|a + \text{H.c.})\right], \\ V_+ &= \frac{\Omega}{2}e^{i\Delta_L t}\sum_{k=1,2}(-1)^{k-1}|g\rangle_k\langle e|. \end{aligned} \tag{12}$$

Here $g_{\rm eff} = 3gU^2V$, $V_- = V_+^\dagger$, H_g (H_e) represents the interaction inside the ground-state (excited-state) subspace, and V_+ denotes the deexcitation from the excited-state subspace to the ground-state subspace. Note that the high-frequency terms in H_e have been eliminated via RWA. Further, we consider weak driving $\Omega \ll g_{\rm eff}$, such that V_+ (V_-) can be treated as a perturbation to the system. By adiabatically eliminating the excited states, the effective Hamiltonian and Lindblad operators describing, respectively, the ground-state subspace and its dissipative processes can be obtained via the effective operator formalism [53,67–70]. The effective Hamiltonian is given by

$$H_{\rm eff} = \frac{\Omega_{\rm MW}}{\sqrt{2}}(|T\rangle\langle\psi_{gg}| + |T\rangle\langle\psi_{ff}| + \text{H.c.}), \tag{13}$$

where $|\psi_{gg}\rangle = |gg\rangle|0\rangle_c$, $|\psi_{ff}\rangle = |ff\rangle|0\rangle_c$, $|T\rangle = (|fg\rangle + |gf\rangle)|0\rangle_c/\sqrt{2}$. Clearly, the microwave field ($\Omega_{\rm MW}$) is able to drive the transitions among states $|\psi_{gg}\rangle$, $|\psi_{ff}\rangle$, and $|T\rangle$. Notably, this can ensure that the generation of the steady state is independent of the initial state. In addition, the effective Lindblad operators are derived as

$$\begin{aligned} L'_{g_1} &= r_\gamma\left[(|T\rangle - |S\rangle)\left(\frac{1}{2\widetilde{\Delta}_{e_1}}\langle T| + \frac{\widetilde{\Delta}_s}{2\widetilde{G}_1}\langle S|\right) - \frac{\widetilde{\Delta}_s}{\widetilde{g}_1}|gg\rangle\langle gg|\right], \\ L'_{g_2} &= r_\gamma\left[(|T\rangle - |S\rangle)\left(\frac{\widetilde{\Delta}_s}{2\widetilde{G}_1}\langle S| - \frac{1}{2\widetilde{\Delta}_{e_1}}\langle T|\right) - \frac{\widetilde{\Delta}_s}{\widetilde{g}_2}|gg\rangle\langle gg|\right], \\ L'_{f_1} &= \frac{r_\gamma}{\sqrt{2}}\left[-\frac{\widetilde{\Delta}_s}{\widetilde{g}_1}(|T\rangle + |S\rangle)\langle gg| + |ff\rangle\left(\frac{1}{\widetilde{\Delta}_{e_1}}\langle T| + \frac{\widetilde{\Delta}_s}{\widetilde{G}_1}\langle S|\right)\right], \\ L'_{f_2} &= \frac{r_\gamma}{\sqrt{2}}\left[\frac{\widetilde{\Delta}_s}{\widetilde{g}_1}(|T\rangle - |S\rangle)\langle gg| - |ff\rangle\left(\frac{1}{\widetilde{\Delta}_{e_1}}\langle T| - \frac{\widetilde{\Delta}_s}{\widetilde{G}_1}\langle S|\right)\right], \\ L'_a &= r_\kappa g_{\rm eff}\left\{\left[\frac{(\widetilde{\Delta}_{e_1} - \widetilde{\Delta}_{e_2})\widetilde{\Delta}_s}{\widetilde{g}_1\widetilde{g}_2}|S\rangle - \frac{\omega_f\widetilde{\Delta}_s}{\widetilde{g}_1\widetilde{g}_2}|T\rangle\right]\langle gg| \right. \\ &\quad \left. - \frac{2}{\widetilde{G}_1}|ff\rangle\langle S|\right\}, \end{aligned} \tag{14}$$

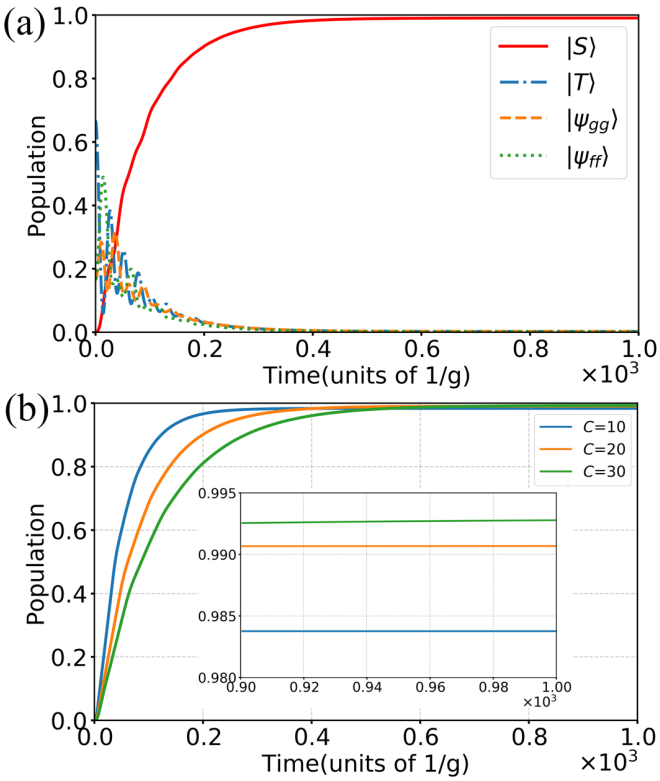

FIG. 5. (a) Populations of $|S\rangle$, $|T\rangle$, $|\psi_{gg}\rangle$, and $|\psi_{ff}\rangle$ versus time. The initial state is set as a mixed state $(|\psi_{gg}\rangle\langle\psi_{gg}| + |\psi_{ff}\rangle\langle\psi_{ff}| + |T\rangle\langle T|)/3$. The parameters are $r_p = 1$, $\omega_f = \omega_{\rm MW} = 0.1g$, $\Delta_e^{(3)} = 150g'_{\rm eff} + \omega_f$, $\Delta_s = \Delta_e^{(3)} - \omega_f$, $\Delta_L = \Delta_e^{(3)} - g_{\rm eff}$, $C = 20$, $\kappa = \gamma/2$, $\Omega = 0.7\gamma$, and $\Omega_{\rm MW} = 0.5\Omega$. (b) Population of $|S\rangle$ versus time for $C = 10$, 20, and 30 (from top to bottom). The inset shows a close-up view of the steady-state populations for $C = 10$, 20, and 30 (from bottom to top). Other common parameters are the same as in (a).

where $r_{\widetilde{\gamma}(\kappa)} = e^{-i\Delta_L t}\Omega\sqrt{\gamma(\kappa)}/2\sqrt{2}$, $\widetilde{\Delta}_{e_1} = \Delta_e^{(3)} - \Delta_L - i\gamma/2$, $\widetilde{\Delta}_{e_2} = \Delta_e^{(3)} + \Delta_f - \Delta_L - i\gamma/2$, $\widetilde{\Delta}_s = \Delta_s + \omega_f - \Delta_L - i\kappa/2$, $\widetilde{g}_{1(2)} = g_{\rm eff}^2 - \widetilde{\Delta}_s\widetilde{\Delta}_{e_{1(2)}}$, and $\widetilde{G}_{1(2)} = 2g_{\rm eff}^2 - \widetilde{\Delta}_s\widetilde{\Delta}_{e_{1(2)}}$. In Eq. (14) the state $|S\rangle$ expressed as $|fg\rangle - |gf\rangle)|0\rangle_c/\sqrt{2}$ can be transformed to the desired maximally entangled state $(|fg\rangle - |gf\rangle)/\sqrt{2}$ after performing a partial trace over the cavity mode degrees of freedom. According to the analytical results above, the underlying dynamics of the dissipative system could be understood as follows: the effective Hamiltonian $H_{\rm eff}$ drives the populations from both $|\psi_{gg}\rangle$ and $|\psi_{ff}\rangle$ to $|T\rangle$, which then can be transferred to $|S\rangle$ via two effective spontaneous emission processes with an identical rate of $|r_\gamma/(2\widetilde{\Delta}_{e_1})|^2$. Simultaneously, populations leakage from $|S\rangle$ through an effective cavity decay with a rate of $|2r_\kappa g_{\rm eff}/\widetilde{G}_1|^2$ also exists, resulting in a slight reduction of fidelity.

In Fig. 5(a) we plot the populations of states $|S\rangle$, $|T\rangle$, $|\psi_{gg}\rangle$, and $|\psi_{ff}\rangle$ versus time by numerically solving the standard Lindblad master equation [Eq. (B4)]. The results show that the population of the target state $|S\rangle$ would be higher than 99% at a time of $500/g$ when the cooperativity is set as $C = 20$. For smaller C, the preparation time for the target state becomes shorter, but the steady-state population is lower due to relatively stronger dissipation, as shown in Fig. 5(b). Although specific experimental parameters for the multiphoton model with $N = 3$ have not been demonstrated, theoretical research on the multiphoton interaction has made some progress, which enables us to anticipate the experimentally feasible parameters to a reasonable extent. Recent studies have made it possible to achieve the nonperturbative ultrastrong two-photon coupling in a superconducting circuit where the two-photon coupling strength becomes comparable to the resonator frequency [22,71] (see Sec. V for detailed discussions). This implies that a two-photon coupling parameter of several hundreds of MHz could be achievable in view of a typical superconducting cavity frequency of ∼GHz [61,72]. Considering a potential weakening in the coupling strength for higher nonlinear process with $N = 3$, we estimate roughly a set of parameters $\{g, \kappa, \gamma\}=2\pi \times \{9.5, 1.5, 3\}$ MHz as an example, corresponding to $C \sim 20$. In this case, the time for reaching steady-state entanglement with the current protocol is estimated as roughly 8 μs.

In above numerical simulations, the parameter r_p is set as 1. In principle, a further increase in the fidelity can be expected by means of increasing r_p, which in turn leads to an overall increase in system parameters. Taking $r_p = 3$ as an example, the effective coupling strength for $N = 3$ can exceed $10^3 g$, corresponding to the detunings $\Delta_s > 10^5 g$ and $\Delta_p > 10^7 g$, which are difficult to satisfy in some physical systems [20,37]. In addition, we note that a large r_p up to 3 is necessary for generating high-fidelity (>0.99) entanglement in the scheme with $N = 1$, which requires very large driving field amplitude, i.e., $\epsilon_0 > 10^6 g$. In our scheme with $N = 3$, prominent enhancement in the atom-field coupling can be realized for $r_p = 1$, and then ϵ_0 is as low as $\sim 10^3 g$. The effective cooperativity, given by $C' = g_{\rm eff}^2/(\kappa\gamma)$, can be enhanced accordingly, resulting in a high-fidelity entanglement preparation. Optimizing our scheme towards fast and high-fidelity entanglement generation could be a promising topic of future study. For instance, potential schemes using quantum feedback control or pulse modulation based on Lyapunov control have been demonstrated in Refs. [47,73–75].

V. DISCUSSION AND CONCLUSION

The proposed scheme could be implemented in contemporary circuit QED systems, where superconducting qubits with Josephson junctions acting as artificial atoms are strongly coupled with an inductance or capacitance resonator or coplanar waveguide resonator [76–78]. The three-level-system transitions can be constructed by charge, transmon, xmon, and flux qubit circuits [79] and engineered by tuning some external parameters (e.g., voltage or magnetic bias). Regarding the multiphoton interactions, it has been demonstrated that the nonlinear Hamiltonian can appear, at least for two-photon interaction (i.e., $N = 2$), in superconducting quantum circuits (SQCs) [20,22,71,80,81]. In particular, nonperturbative two-photon interactions with substantial coupling strengths have been realized in Refs. [22,71], which are distinct from the perturbative cases where higher-order effects of a dipolar interaction enable small effective coupling strengths [17,18]. It is worth noting that for perturbative multiphoton processes the coupling coefficient would decrease with increasing N.

Nevertheless, as described in Refs. [22,71], the nonperturbative two-photon interaction could be naturally implemented with tunable coupling strength, thus enabling the two-photon coupling strength to be comparable to the bare one-photon coupling. Even so, the feasibility of the nonperturbative two-photon interactions and the method to expand it for general multiphoton processes remains open, which should motivate further research on this topic. In addition, the required parametric driving can be implemented by modulating the flux through a cavity-embedded superconducting quantum interference device (SQUID) [61,82,83]. Other solid-state implementations like nitrogen-vacancy (NV) centers in diamond coupled with a whispering-gallery-mode (WGM) cavity are also possible applications for our scheme [84,85].

In conclusion, we have demonstrated the enhancement of atom-field coupling in a multiphoton TC system driven by a parametric driving field. By choosing proper parameters with respect to the odevity of N, the original N-photon atom-cavity interaction can be reduced to effective single- or two-photon interaction, with the effective interaction being significantly enhanced. The effective atom-cavity coupling strength can be enhanced to be N-dependent on top of the exponential enhancement induced only by the parametric driving. Moreover, we show that the detrimental effects of dissipation on systematic evolution can be mitigated with increasing N. Practical application in the preparation of high-fidelity maximally entangled steady state has also been demonstrated. We expect that our proposal could find wide applications in quantum information protocols.

ACKNOWLEDGMENTS

All authors would like to thank the anonymous referees for constructive comments that were helpful for improving the quality of the work. This work was supported by National Natural Science Foundation of China (NSFC) (Grant No. 11675046), Program for Innovation Research of Science in Harbin Institute of Technology (A20141y2), and Postdoctoral Scientific Research Developmental Fund of Heilongjiang Province (LBH-Q15060).

APPENDIX A: DERIVATION OF THE EFFECTIVE HAMILTONIAN

To understand the potential properties of our system, it is convenient to derive the effective Hamiltonian. We first perform a unitary transformation with $U^{(N)} = \exp[-i\omega_p(a^\dagger a + N\sum_{k=1}^{2}|e\rangle_k\langle e|)t]$ on Eq. (1), and assume $\theta_p = 0$ for mathematical simplicity. To diagonalize the cavity-only part in the resulting Hamiltonian, we further perform a squeezing transformation with $U_S = \exp[r_p(a^2 - a^{\dagger 2})/2]$, where the squeeze parameter is defined via $r_p = (1/2)\mathrm{arctanh}(2\epsilon_0/\Delta_p)$. In this case, the total Hamiltonian of the system in the squeezed reference frame is described by

$$H' = H_{\mathrm{ACS}}^{(N)} + H'_{\mathrm{CL}} + H_{\mathrm{MW}}, \tag{A1}$$

where

$$H'_{\mathrm{CL}} = \frac{\Omega}{2}e^{i\Delta_L t}\sum_{k=1,2}(-1)^{k-1}|g\rangle_k\langle e| + \mathrm{H.c.}, \tag{A2}$$

and H_{MW} remains unchanged during the calculations. In Eq. (A2) $\Delta_L = \omega - N\omega_p$. As for $H_{\mathrm{ACS}}^{(N)}$, it can be reduced to either an effective single- or two-photon TC Hamiltonian for arbitrary N by choosing proper parameter conditions. In the following, we give the concrete expressions for cases of $N = 1, 2, 3, 4$, which are enough to deduce the desired effective Hamiltonian. The corresponding results are given, respectively, by

$$H_{\mathrm{ACS}}^{(1)} = \Delta_s a^\dagger a + \sum_{k=1,2}\left[\Delta_e^{(1)}|e\rangle_k\langle e| + \omega_f|f\rangle_k\langle f| + g(U|e\rangle_k\langle f|a - V|e\rangle_k\langle f|a^\dagger + \mathrm{H.c.})\right], \tag{A3a}$$

$$H_{\mathrm{ACS}}^{(2)} = \Delta_s a^\dagger a + \sum_{k=1,2}\left\{\Delta_e^{(2)}|e\rangle_k\langle e| + \omega_f|f\rangle_k\langle f| + g[U^2|e\rangle_k\langle f|a^2 + V^2|e\rangle_k\langle f|(a^\dagger)^2 - UV|e\rangle_k\langle f|(a^\dagger a + aa^\dagger) + \mathrm{H.c.}]\right\}, \tag{A3b}$$

$$H_{\mathrm{ACS}}^{(3)} = \Delta_s a^\dagger a + \sum_{k=1,2}\left\{\Delta_e^{(3)}|e\rangle_k\langle e| + \omega_f|f\rangle_k\langle f| + g[U^3|e\rangle_k\langle f|a^3 - V^3|e\rangle_k\langle f|(a^\dagger)^3 + UV^2|e\rangle_k\langle f|(a^\dagger a^\dagger a + aa^\dagger a^\dagger + a^\dagger aa^\dagger)\right.$$
$$\left.\underline{-U^2V|e\rangle_k\langle f|(aaa^\dagger + a^\dagger aa + aa^\dagger a)} + \mathrm{H.c.}]\right\}, \tag{A3c}$$

$$H_{\mathrm{ACS}}^{(4)} = \Delta_s a^\dagger a + \sum_{k=1,2}\left\{\Delta_e^{(4)}|e\rangle_k\langle e| + \omega_f|f\rangle_k\langle f| + g[U^4|e\rangle_k\langle f|a^4 + V^4|e\rangle_k\langle f|(a^\dagger)^4\right.$$
$$- UV^3|e\rangle_k\langle f|(aa^\dagger a^\dagger a^\dagger + a^\dagger aa^\dagger a^\dagger + a^\dagger a^\dagger aa^\dagger + a^\dagger a^\dagger a^\dagger a)\underline{-U^3V|e\rangle_k\langle f|(a^\dagger aaa + aa^\dagger aa + aaa^\dagger a + aaaa^\dagger)}$$
$$\left.+ U^2V^2|e\rangle_k\langle f|(aa^\dagger a^\dagger a + aaa^\dagger a^\dagger + a^\dagger aaa^\dagger + a^\dagger a^\dagger aa + aa^\dagger aa^\dagger + a^\dagger aa^\dagger a) + \mathrm{H.c.}]\right\}, \tag{A3d}$$

where $\Delta_s = \Delta_p\mathrm{sech}(2r_p)$ with $\Delta_p = \omega_0 - \omega_p$, $\Delta_e^{(N)} = \omega_e - N\omega_p$, $U = \cosh(r_p)$, and $V = \sinh(r_p)$.

For odd N (i.e., $N_o = 1, 3, \ldots$), adjusting $\Delta_e^{(N_o)} - \omega_f = \Delta_s$, the rotating term describing the effective single-photon process [e.g., the underlined term in Eq. (A3c)] is resonant while the other terms are off-resonant and hence could be neglected via RWA. Similarly, for even N (i.e., $N_e = 2, 4, \ldots$), the rotating term describing the effective two-photon process [annihilating two photons with a transition of the atom from the ground state to excited state; see, e.g., the underlined term

in Eq. (A3d)] continues on condition that $\Delta_e^{(N_e)} - \omega_f = 2\Delta_s$. In other words, the N-photon TC Hamiltonian can be reduced to either an effective single- or two-photon TC Hamiltonian in terms of the odevity of the photon number N. By carefully comparing and deriving the exact form of $H_{\rm ACS}^{(N)}$ for various N, we obtain the effective form of the reduced single- and two-photon TC Hamiltonians

$$H_{\rm ACS}^{(N_o)} = \Delta_s a^\dagger a + \sum_{k=1,2}\Big\{\Delta_e^{(N_o)}|e\rangle_k\langle e| + \omega_f|f\rangle_k\langle f| + (-V)^m U^{m+1} g|e\rangle_k\langle f| \sum_l P_l[a^{m+1}(a^\dagger)^m] + \text{H.c.}\Big\}, \tag{A4a}$$

$$H_{\rm ACS}^{(N_e)} = \Delta_s a^\dagger a + \sum_{k=1,2}\Big\{\Delta_e^{(N_e)}|e\rangle_k\langle e| + \omega_f|f\rangle_k\langle f| + (-V)^n U^{n+2} g|e\rangle_k\langle f| \sum_l P_l[a^{n+2}(a^\dagger)^n] + \text{H.c.}\Big\}, \tag{A4b}$$

which are valid for

$$\Delta_e^{(N_o)} - \omega_f = \Delta_s, \quad \Delta_e^{(N_e)} - \omega_f = 2\Delta_s. \tag{A5}$$

In Eq. (A4) $m = \frac{N_o-1}{2}$, $n = \frac{N_e-2}{2}$, and the sum with respect to l is over all permutations (produced by the permutation operator P_l).

APPENDIX B: DERIVATION OF THE MASTER EQUATION

The cavity mode in the squeezed frame is coupled to a squeezed vacuum reservoir if initially the cavity mode in the laboratory frame is coupled to a vacuum reservoir. To eliminate the additional noise [as characterized by N_s and M_s in the master equation (10)] and ensure the system in vacuum in the squeezed frame, we introduce an auxiliary squeezed field (which can be thought of as a squeezed vacuum reservoir) to drive the cavity in the laboratory frame. We note that this method has been demonstrated in Refs. [45–48] and generalized in our recent studies [56,57], in which more details can be seen clearly.

Here we give a brief derivation of the master equation in the presence of squeezed reservoir. After introducing the auxiliary squeezed reservoir (with a squeezing parameter r_e and a reference phase θ_e) in the laboratory frame, the master equation describing the dynamics of the system can be written as

$$\dot\rho = i[\rho, H] + \sum_{z,k}\mathcal{L}(L_{zk})\rho + (N_l+1)\mathcal{L}(L_a)\rho + N_l\mathcal{L}(L_a^\dagger)\rho - M_l\mathcal{L}'(L_a^\dagger)\rho - M_l^*\mathcal{L}'(L_a)\rho, \tag{B1}$$

where $N_l = \sinh^2(r_e)$ and $M_l = \cosh(r_e)\sinh(r_e)e^{i\theta_e}$ are parameters that describe the squeezed vacuum reservoir. In the squeezed frame, the above master equation is reexpressed as

$$\dot\rho = i[\rho, H'] + \sum_{z,k}\mathcal{L}(L_{zk})\rho + (N_s'+1)\mathcal{L}(L_a)\rho + N_s'\mathcal{L}(L_a^\dagger)\rho - M_s'\mathcal{L}'(L_a^\dagger)\rho - M_s'^*\mathcal{L}'(L_a)\rho, \tag{B2}$$

where N_s' and M_s' are given, respectively, by

$$N_s' = \sinh^2(r_e)\cosh(2r_p) + \sinh^2(r_p) + \tfrac{1}{2}\sinh(2r_e)\sinh(2r_p)\cos(\theta_e+\theta_p), \tag{B3a}$$

$$M_s' = \exp(i\theta_p)\big(\tfrac{1}{2}\sinh(2r_p)\cosh(2r_e) + \tfrac{1}{2}\sinh(2r_e)\{\exp[i(\theta_e+\theta_p)]\cosh^2(r_p) + \exp[-i(\theta_e+\theta_p)]\sinh^2(r_p)\}\big). \tag{B3b}$$

By choosing $r_e = r_p$ and $\theta_e + \theta_p = \pi$, we have $N_s' = M_s' = 0$, and in this way the master equation (B2) is simplified to the standard Lindblad form

$$\dot\rho = i[\rho, H'] + \sum_{z,k}\mathcal{L}(L_{zk})\rho + \mathcal{L}(L_a)\rho. \tag{B4}$$

[1] B. W. Shore and P. L. Knight, J. Mod. Opt. **40**, 1195 (1993).
[2] J. Casanova, G. Romero, I. Lizuain, J. J. García-Ripoll, and E. Solano, Phys. Rev. Lett. **105**, 263603 (2010).
[3] S. J. D. Phoenix and P. L. Knight, Phys. Rev. A **44**, 6023 (1991).
[4] G.-C. Guo and S.-B. Zheng, Phy. Lett. A **223**, 332 (1996).
[5] P. Góra and C. Jedrzejek, Phys. Rev. A **45**, 6816 (1992).
[6] A. Smirne, H.-P. Breuer, J. Piilo, and B. Vacchini, Phys. Rev. A **82**, 062114 (2010).
[7] M. D. Crisp, Phys. Rev. A **43**, 2430 (1991).
[8] S. Singh, Phys. Rev. A **25**, 3206 (1982).
[9] C. Sukumar and B. Buck, Phys. Lett. A **83**, 211 (1981).
[10] F. L. Kien, M. Kozierowski, and T. Quang, Phys. Rev. A **38**, 263 (1988).
[11] C. J. Villas-Boas and D. Z. Rossatto, Phys. Rev. Lett. **122**, 123604 (2019).
[12] B. Buck and C. Sukumar, Phys. Lett. A **81**, 132 (1981).
[13] C. C. Gerry, Phys. Rev. A **37**, 2683 (1988).
[14] A. Joshi and R. R. Puri, Phys. Rev. A **45**, 5056 (1992).
[15] D. J. Gauthier, Q. Wu, S. E. Morin, and T. W. Mossberg, Phys. Rev. Lett. **68**, 464 (1992).
[16] M. Brune, J. M. Raimond, P. Goy, L. Davidovich, and S. Haroche, Phys. Rev. Lett. **59**, 1899 (1987).
[17] W. Vogel and R. L. de Matos Filho, Phys. Rev. A **52**, 4214 (1995).
[18] D. M. Meekhof, C. Monroe, B. E. King, W. M. Itano, and D. J. Wineland, Phys. Rev. Lett. **76**, 1796 (1996).
[19] F. Deppe, M. Mariantoni, E. Menzel, A. Marx, S. Saito, K. Kakuyanagi, H. Tanaka, T. Meno, K. Semba, H. Takayanagi *et al.*, Nat. Phys. **4**, 686 (2008).
[20] P. Neilinger, M. Rehák, M. Grajcar, G. Oelsner, U. Hübner, and E. Il'ichev, Phys. Rev. B **91**, 104516 (2015).
[21] L. Garziano, R. Stassi, V. Macrì, A. F. Kockum, S. Savasta, and F. Nori, Phys. Rev. A **92**, 063830 (2015).

[22] S. Felicetti, D. Z. Rossatto, E. Rico, E. Solano, and P. Forn-Díaz, Phys. Rev. A **97**, 013851 (2018).
[23] M. Tavis and F. W. Cummings, Phys. Rev. **170**, 379 (1968).
[24] M. Tavis and F. W. Cummings, Phys. Rev. **188**, 692 (1969).
[25] S. Agarwal, S. M. Hashemi Rafsanjani, and J. H. Eberly, Phys. Rev. A **85**, 043815 (2012).
[26] M. S. Abdalla, S. S. Hassan, and A. S. F. Obada, Phys. Rev. A **34**, 4869 (1986).
[27] J. H. Zou, T. Liu, M. Feng, W. L. Yang, C. Y. Chen, and J. Twamley, New J. Phys. **15**, 123032 (2013).
[28] C. Genes, P. R. Berman, and A. G. Rojo, Phys. Rev. A **68**, 043809 (2003).
[29] A. Retzker, E. Solano, and B. Reznik, Phys. Rev. A **75**, 022312 (2007).
[30] J. M. Fink, R. Bianchetti, M. Baur, M. Göppl, L. Steffen, S. Filipp, P. J. Leek, A. Blais, and A. Wallraff, Phys. Rev. Lett. **103**, 083601 (2009).
[31] W. K. Wootters, Phys. Rev. Lett. **80**, 2245 (1998).
[32] T. E. Tessier, I. H. Deutsch, A. Delgado, and I. Fuentes-Guridi, Phys. Rev. A **68**, 062316 (2003).
[33] I. Kudryavtsev, A. Lambrecht, H. Moya-Cessa, and P. Knight, J. Mod. Opt. **40**, 1605 (1993).
[34] G.-F. Zhang and Z.-Y. Chen, Opt. Commun. **275**, 274 (2007).
[35] E. K. Bashkirov, Phys. Scr. **82**, 015401 (2010).
[36] S.-B. Zheng and G.-C. Guo, Phys. Rev. Lett. **85**, 2392 (2000).
[37] A. Blais, R.-S. Huang, A. Wallraff, S. M. Girvin, and R. J. Schoelkopf, Phys. Rev. A **69**, 062320 (2004).
[38] D. W. Vernooy, A. Furusawa, N. P. Georgiades, V. S. Ilchenko, and H. J. Kimble, Phys. Rev. A **57**, R2293 (1998).
[39] C. Qian, X. Xie, J. Yang, K. Peng, S. Wu, F. Song, S. Sun, J. Dang, Y. Yu, M. J. Steer *et al.*, Phys. Rev. Lett. **122**, 087401 (2019).
[40] A. Bisht, J. Cuadra, M. Wersall, A. Canales, T. J. Antosiewicz, and T. Shegai, Nano Lett. **19**, 189 (2019).
[41] B. Gurlek, V. Sandoghdar, and D. Martin-Cano, ACS Photonics **5**, 456 (2018).
[42] X. Yu, Y. Yuan, J. Xu, K.-T. Yong, J. Qu, and J. Song, Laser Photonics Rev. **13**, 1800219 (2019).
[43] L. Garziano, V. Macrì, R. Stassi, O. Di Stefano, F. Nori, and S. Savasta, Phys. Rev. Lett. **117**, 043601 (2016).
[44] S. Haroche, Rev. Mod. Phys. **85**, 1083 (2013).
[45] C. Leroux, L. C. G. Govia, and A. A. Clerk, Phys. Rev. Lett. **120**, 093602 (2018).
[46] W. Qin, A. Miranowicz, P.-B. Li, X.-Y. Lü, J. Q. You, and F. Nori, Phys. Rev. Lett. **120**, 093601 (2018).
[47] Y.-H. Chen, W. Qin, and F. Nori, Phys. Rev. A **100**, 012339 (2019).
[48] X.-Y. Lü, Y. Wu, J. R. Johansson, H. Jing, J. Zhang, and F. Nori, Phys. Rev. Lett. **114**, 093602 (2015).
[49] M.-A. Lemonde, N. Didier, and A. A. Clerk, Nat. Commun. **7**, 11338 (2016).
[50] Y.-L. Zhang, C.-L. Zou, C.-S. Yang, H. Jing, C.-H. Dong, G.-C. Guo, and X.-B. Zou, New J. Phys. **20**, 093005 (2018).
[51] W. Qin, V. Macrì, A. Miranowicz, S. Savasta, and F. Nori, Phys. Rev. A **100**, 062501 (2019).
[52] A. S. Sørensen and K. Mølmer, Phys. Rev. Lett. **91**, 097905 (2003).
[53] M. J. Kastoryano, F. Reiter, and A. S. Sørensen, Phys. Rev. Lett. **106**, 090502 (2011).
[54] F. Mallet, M. A. Castellanos-Beltran, H. S. Ku, S. Glancy, E. Knill, K. D. Irwin, G. C. Hilton, L. R. Vale, and K. W. Lehnert, Phys. Rev. Lett. **106**, 220502 (2011).
[55] U. L. Andersen, T. Gehring, C. Marquardt, and G. Leuchs, Phys. Scr. **91**, 053001 (2016).
[56] Y. Wang, C. Li, E. M. Sampuli, J. Song, Y. Jiang, and Y. Xia, Phys. Rev. A **99**, 023833 (2019).
[57] Y. Wang, J.-L. Wu, J. Song, Y.-Y. Jiang, Z.-J. Zhang, and Y. Xia, Ann. Phys. **531**, 1900220 (2019).
[58] H. Vahlbruch, M. Mehmet, S. Chelkowski, B. Hage, A. Franzen, N. Lastzka, S. Goßler, K. Danzmann, and R. Schnabel, Phys. Rev. Lett. **100**, 033602 (2008).
[59] H. Vahlbruch, M. Mehmet, K. Danzmann, and R. Schnabel, Phys. Rev. Lett. **117**, 110801 (2016).
[60] R. Schnabel, Phys. Rep. **684**, 1 (2017).
[61] S. Kono, Y. Masuyama, T. Ishikawa, Y. Tabuchi, R. Yamazaki, K. Usami, K. Koshino, and Y. Nakamura, Phys. Rev. Lett. **119**, 023602 (2017).
[62] K. Murch, S. Weber, K. Beck, E. Ginossar, and I. Siddiqi, Nature (London) **499**, 62 (2013).
[63] D. M. Toyli, A. W. Eddins, S. Boutin, S. Puri, D. Hover, V. Bolkhovsky, W. D. Oliver, A. Blais, and I. Siddiqi, Phys. Rev. X **6**, 031004 (2016).
[64] A. Bienfait, P. Campagne-Ibarcq, A. H. Kiilerich, X. Zhou, S. Probst, J. J. Pla, T. Schenkel, D. Vion, D. Esteve, J. J. L. Morton *et al.*, Phys. Rev. X **7**, 041011 (2017).
[65] J. Johansson, P. Nation, and F. Nori, Comput. Phys. Commun. **184**, 1234 (2013).
[66] H.-P. Breuer and F. Petruccione, *The Theory of Open Quantum Systems* (Oxford University Press, New York, 2002), Chap. 3.
[67] F. Reiter and A. S. Sørensen, Phys. Rev. A **85**, 032111 (2012).
[68] L.-T. Shen, X.-Y. Chen, Z.-B. Yang, H.-Z. Wu, and S.-B. Zheng, Phys. Rev. A **84**, 064302 (2011).
[69] S.-L. Su, X.-Q. Shao, H.-F. Wang, and S. Zhang, Phys. Rev. A **90**, 054302 (2014).
[70] X.-Q. Shao, T.-Y. Zheng, C. H. Oh, and S. Zhang, Phys. Rev. A **89**, 012319 (2014).
[71] S. Felicetti, M.-J. Hwang, and A. Le Boité, Phys. Rev. A **98**, 053859 (2018).
[72] X. Han, C.-L. Zou, and H. X. Tang, Phys. Rev. Lett. **117**, 123603 (2016).
[73] J. Song, Z.-J. Zhang, Y. Xia, X.-D. Sun, and Y.-Y. Jiang, Opt. Express **24**, 21674 (2016).
[74] Y.-H. Chen, Z.-C. Shi, J. Song, Y. Xia, and S.-B. Zheng, Phys. Rev. A **97**, 032328 (2018).
[75] Y.-H. Chen, Z.-C. Shi, J. Song, Y. Xia, and S.-B. Zheng, Phys. Rev. A **96**, 043853 (2017).
[76] I. Chiorescu, P. Bertet, K. Semba, Y. Nakamura, C. Harmans, and J. Mooij, Nature (London) **431**, 159 (2004).
[77] J. Q. You, Y.-x. Liu, and F. Nori, Phys. Rev. Lett. **100**, 047001 (2008).
[78] J. You and F. Nori, Nature (London) **474**, 589 (2011).
[79] X. Gu, A. F. Kockum, A. Miranowicz, Y.-X. Liu, and F. Nori, Phys. Rep. **718**, 1 (2017).
[80] J. Hauss, A. Fedorov, C. Hutter, A. Shnirman, and G. Schön, Phys. Rev. Lett. **100**, 037003 (2008).

[81] P. Bertet, I. Chiorescu, G. Burkard, K. Semba, C. J. P. M. Harmans, D. P. DiVincenzo, and J. E. Mooij, Phys. Rev. Lett. **95**, 257002 (2005).

[82] T. Yamamoto, K. Inomata, M. Watanabe, K. Matsuba, T. Miyazaki, W. D. Oliver, Y. Nakamura, and J. S. Tsai, Appl. Phys. Lett. **93**, 042510 (2008).

[83] L. Zhong, E. P. Menzel, R. D. Candia, P. Eder, M. Ihmig, A. Baust, M. Haeberlein, E. Hoffmann, K. Inomata, T. Yamamoto *et al.*, New J. Phys. **15**, 125013 (2013).

[84] P.-B. Li, S.-Y. Gao, and F.-L. Li, Phys. Rev. A **83**, 054306 (2011).

[85] C.-H. Li and P.-B. Li, Phys. Rev. A **97**, 052319 (2018).